JOURNAL OF MATERIALS SCIENCE 24 (1989) 333–338

Ionic conductivity of synthetic analcime, sodalite and offretite

GABRIELE KELEMEN, WOLFGANG LORTZ*, GÜNTER SCHÖN
Institut für Anorganische Chemie der Universität Essen, Schützenbahn 70, D-4300 Essen 1, West Germany

The ionic conductivity of pressed pellets of dehydrated synthetic analcime, sodalite and offretite was determined by a.c. measurements within the range 10 Hz to 10 MHz. The ionic conductivity values of those zeolites exchanged with various monovalent cations were determined by the complex impedance plane method. The conduction activation energies range between 63 and 101 kJ mol^{-1}. Sodium analcime shows the best ionic conductivity, namely $1.8 \times 10^{-4}\,\Omega^{-1}\,cm^{-1}$ at 400° C. A comparison with the conductivity of other ion-conducting solids was made.

1. Introduction

There is still a great need for new solid materials that have a high conductivity of alkali ions. These solid electrolytes are used, for instance, as ion-conduction membranes in electrochemical batteries and as probes or sensors in process control and analytical chemistry.

It is very difficult to make *a priori* reliable predictions about the value of the ionic conductivity in a material with known crystal structure. In the search for new fast ionic conductors there are some guidelines which help to determine the structural characteristics that promote high ionic conductivity. A prerequisite for high ionic conductivity in solid electrolytes is a large number of empty sites available for the mobile ions to jump into. The structure should have open channels and cavities through which mobile ions may migrate. The size and charge of mobile ions play an important role and there must be a low activation energy barrier for the jumping ions between neighbouring sites. These structural characteristics for a high diffusion velocity of ions show among others zeolites with exchangeable cations.

Several researchers have investigated the ionic conductivity of zeolites [1–6]. Most of them used the commercially available zeolites A, X, and Y. In the case of the dehydrated zeolites X and Y with their large cavities and wide channels the mobile cations tend to stick at sites in the cavities and channel walls because of relatively high coulombic interactions. In the hydrated state the ionic conductivity is far from that of fast ionic conductors because of the relatively immobile large hydrated complexes in which the cations are usually present. Only a small proportion of the approximately 140 different synthetic zeolites has been investigated with respect to its suitability for solid electrolyte.

It was thus considered worthwhile to study the electrical conductivity of zeolites with more compact structures by means of low frequency a.c. measurements. To this end we chose sodalite and analcime which are zeolites with narrow channel systems and offretite with a medium-sized free diameter in its channel system. Analcime possesses a one-dimensional channel system with non-intersecting channels. The free diameter of the smallest apertures in hydrated analcime is 0.26 nm. The smallest openings in the three-dimensional channel system of sodalite are the six-membered oxygen rings of sodalite cages with an active diameter of 0.23 nm in the hydrated state. In the three-dimensional channel system of offretite a 0.64 nm channel runs parallel to the c axis intersecting two smaller channels formed by eight rings with a free cross-section of $0.36 \times 0.52\,nm^2$ in the hydrated state. These zeolites were synthesized with different monovalent cations or were ion-exchanged, respectively, to obtain the intended cation form. Investigations on the influence of several parameters, such as the cation type, Si/Al ratio and the dimensions of the internal framework, yield information which make it possible to modify zeolites in such a way as to improve their ionic conductivity.

2. Experimental details

2.1. Synthesis and ion exchange

Sodalite, analcime and offretite were prepared by crystallization from alkaline solutions and hydrogels, respectively, mostly in Teflon-lined stainless steel autoclaves at temperatures between 50 and 300° C. A detailed description of the autoclaves used and of the synthesis conditions for the preparation of sodalite and analcime is given by Lortz [7]. Offretite was synthesized with reference to Raeder [8]. Our starting materials for the offretite synthesis were NaOH, KOH, and aluminium strip (p.a. Merck), SiO_2 sol (40 wt % Ludox HS40, Du Pont) and $(CH_3)_4NOH$ (25 wt % in water, Fluka). This offretite contains in its synthesized form three monovalent cations which are TMA^+ (tetramethylammonium), K^+ and Na^+. The

* *Present address.* Degussa AG, Rodenbacher Chaussee 4, 6450 Hanau 1, West Germany.

0022–2461/89 $03.00 + .12

TABLE I Summary of the synthesized and ion exchanged zeolites

Type of zeolite	Si/Al or Ga/Al	Method of ion exchange	Mol per cent ion content
Li-sodalite	1:1	1n $LiNO_3$ solution at 80° C	99 Li
Na-sodalite	1:1	originally synthesized	100 Na
K-sodalite	1:1	1n KNO_3 solution at 80° C	99 K
Rb-sodalite	1:1	1n $RbNO_3$ solution at 80° C	54 Rb
Li-sodalite	5:1	0.1n Li_2CO_3 solution at 80° C	80 Li
Na-sodalite	5:1	0.1n Na_2CO_3 solution at 80° C	99 Na
K-sodalite	5:1	0.1n K_2CO_3 solution at 80° C	99 K
Rb-sodalite	5:1	0.1n Rb_2CO_3 solution at 80° C	97 Rb
Li-Ga-sodalite	1:1	1n $LiNO_3$ solution at 80° C	56 Li
Na-Ga-sodalite	1:1	originally synthesized	100 Na
K-Ga-sodalite	1:1	1n KNO_3 solution at 80° C	36 K
Rb-Ga-sodalite	1:1	1n $RbNO_3$ solution at 80° C	27 Rb
Li-analcime	2.2:1	$LiNO_3$ melt at 300° C with originally synthesized Na-analcime	93 Li
Na-analcime	2.2:1	originally synthesized	100 Na
K-analcime	2.2:1	1n KNO_3 solution, hydrothermal at 200° C with originally synthesized Na-analcime	95 K
Rb-analcime	2.2:1	originally synthesized	100 Rb
Cs-analcime	2.6:1	originally synthesized	100 Cs
Li-offretite	3:1	1n LiCl solution at 80° C	51 Li
Na-offretite	3:1	$NaNO_3$ melt	72 Na
K-offretite	3:1	1n KCl solution at 80° C	98 K
Rb-offretite	3:1	0.1n Rb_2CO_3 solution at 80° C	63 Rb

crystals were separated from the mother liquor by filtration and subsequently washed with distilled water. They were dried in air at 100° C and stored in a desiccator over saturated aqueous $Ca(NO_3)_2$-solution before analysis. Silicon, aluminium and gallium were determined in the classical gravimetric manner. The content of alkali ions was determined by atomic absorption spectrophotometry. In the case of zeolites containing organic cations an organic microanalysis was performed for the determination of carbon, hydrogen and nitrogen. Ion exchange was done by exchange techniques in aqueous solutions or salt melts with our synthesized zeolites as starting materials. Table I summarizes the synthesized and exchanged zeolites, exchange methods and degree of exchange.

The ion exchange in aqueous solutions was carried out at 80° C in PTFE-bottles, which were rotated at 2 r.p.m. 5 g of the zeolite and about 100 ml exchange solution were used in each case. The solution was renewed after about 8 h of exchange. The silicon-rich TMA-sodalite (Si/Al = 5) was transformed into Na-sodalite by the following procedure [7]. Thermal decomposition of TMA^+ ions at 600° C under a stream of nitrogen was followed by ion exchange at 80° C with 0.1N Na_2CO_3 solution, oxidation at 700° C under a stream of oxygen and three times repeated ion exchange with 0.1N Na_2CO_3 solution at 80° C. This Na-sodalite was the starting material for the Li^+, K^+, and Rb^+ ion exchange in the case of silicon-rich sodalites. The thermal decomposition of TMA^+ ions in offretite was carried out at 650° C under a stream of oxygen. It was not possible to completely replace all the cations of the synthesized offretite with Li^+, Na^+, and Rb^+, respectively. K^+ ions, built into the hexagonal prisms of the zeolite framework during synthesis, are not exchangeable or difficult to replace [9].

X-ray diffraction patterns of all the samples showed the characteristic sharp spectrum of each structure with no foreign peaks.

Since it was intended to carry out conduction measurements at temperatures between 100 and 600° C, it was necessary to investigate the thermal stability of all the samples. Differential thermal analysis (DTA) was carried out with Linseis L62 equipment [7, 10] over the temperature range 30 to 1130° C with air surrounding the specimen.

Up to far above 600° C there was no indication of any change in the crystal structure of the zeolites. Fig. 1 shows typical DTA curves of the sodalite series. The endothermic peak in the lower temperature range is due to dehydration. The exothermic breakdown of the crystal structure in the upper temperature range depends on cations and shows a displacement to higher temperatures for larger cations.

2.2. Preparation of compacts

Powder compressed discs with an average diameter of 13 mm and 0.3–0.5 mm thickness were prepared under vacuum with a KBr press. In general, a pressure of 6×10^8 Pa was applied. The pellet density was 70–75% of the crystal density. To increase the mechanical stability, zeolite compacts were heated in air at 400° C for 24 h. There was no indication of any crystal damage in X-ray diffraction patterns after application of pressure and after the heating cycle. A thin layer of

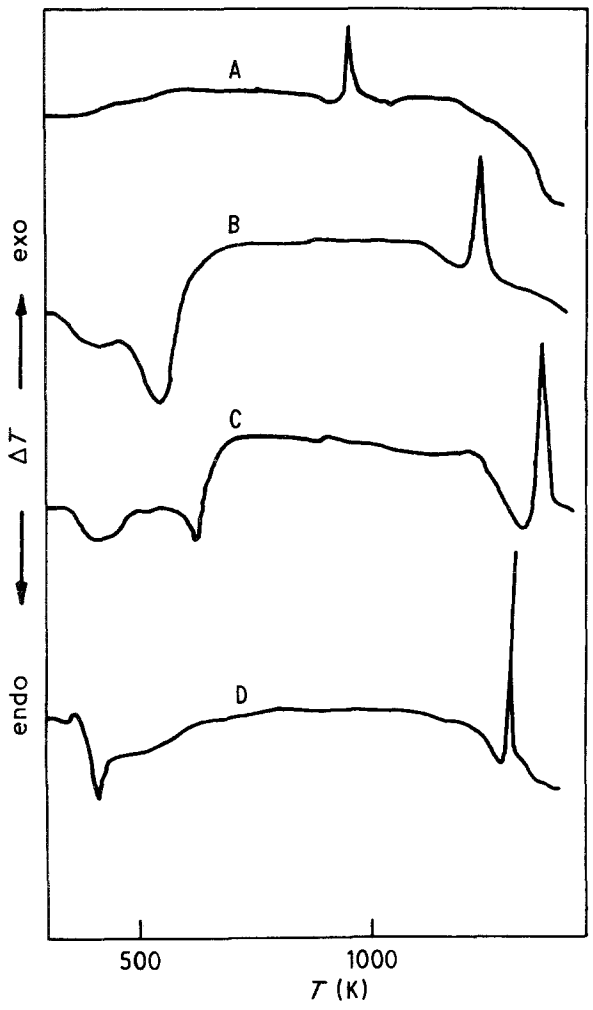

Figure 1 DTA profile of the sodalite series. A Li–sodalite (1 : 1), B Na–sodalite (1 : 1), C K–sodalite (1 : 1), D Rb–sodalite (1 : 1).

platinum (0.1 μm) was vacuum sputtered onto both sides of the compact. The powder compacts were carefully ground to a diameter of 5 mm.

2.3. Procedure

The measuring equipment with the conductivity cell and the data handling is described elsewhere in detail [7, 11]. The pellets inserted into the conductivity cell were heated at 400° C for 1 h under an argon pressure of 10 Pa. The impedance measurements were carried out from 10 Hz to 10 MHz in 300 logarithmic equidistant frequency steps at each temperature using Hewlett Packard LF impedance analyser HP 4192 A. All measurements were carried out in the temperature range between 100 and 600° C at intervals of 25° C. At each interval the temperature was kept constant to $\pm$ 1° C for at least 30 min.

3. Results and discussion

3.1. Interpretation of impedance measurements

One of the frequently used techniques to obtain information on the ionic conductivity of a solid electrolyte is to analyse a.c. measurements in the complex impedance plane (Argand plot). The application of the complex plane method in analysing solid electrolyte measurements was introduced by Bauerle [12]. To simulate solid electrolyte behaviour we chose

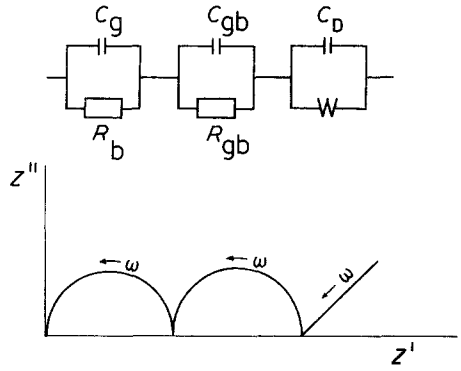

Figure 2 Anticipated equivalent circuit and complex impedance plane plot for polycrystalline specimens with blocking electrodes. W is the Warburg impedance.

the equivalent circuit shown in Fig. 2 for our polycrystalline specimen, using blocking electrodes. The resistance of the polycrystalline material is composed of the bulk crystal resistance (R_b) and the grain boundary resistance (R_{gb}). Polarization effects at the grain boundaries must be considered in the form of a capacitance C_{gb} in parallel with R_{gb}. C_g corresponds to the geometric capacitance of the cell. The parallel arrangement of R_b and C_g in series with the other constituents of the equivalent circuit is a good approximation [7] for our system. There is no discharge or reaction at the electrode–electrolyte interface during a.c. measurements. This interface may be described as a double layer capacitance C_D in series with the sample resistance. In parallel with the double-layer capacitance there is a frequency-dependent impedance, the so-called Warburg impedance. This impedance results in a spike inclined to the normal in the lower frequency range of the complex impedance plane plot (Fig. 2). The commonly accepted interpretation of a spike with a slope of 1 is provided by Warburg [13, 14]. The Warburg concept is based upon the assumption of a diffusive boundary condition at an electrode which blocks an ionic species. However, the available experimental data show a wide range of slope angles for which there is at present no generally accepted model [15, 16].

The impedance spectrum, when plotted on a linear scale, takes the form of a semi-circle for each *RC* element (Fig. 2). A distinct separation into two semi-circles corresponding to the two *RC* elements in our equivalent circuit is only possible if the time constants differ at least by a factor of 100 [17].

Experimentally, semi-circles with centres below the z' axis are often observed. This non-ideal behaviour is due to a distribution of relaxation times in the series of parallel *RC* elements representing the polycrystalline electrolyte [18, 19]. The value of z' at the minimum of z'' in the complex plane plot is in most cases the best estimate for the overall resistance [20]. This overall resistance includes all resistance-causing phenomena such as intragranular and intergranular contributions and is a characteristics parameter when making use of a particular material in solid electrolyte applications.

If there is no distinct minimum in the complex impedance plane plot, curve-fitting techniques [21] or the simulation of the equivalent circuit [22] must be

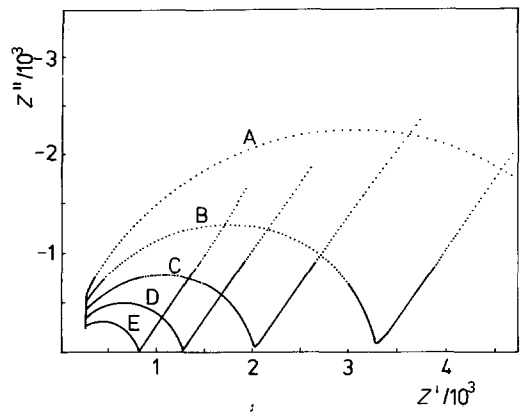

Figure 3 Complex impedance plane plots for analcime. A at 250° C, B at 275° C, C at 300° C, D at 325° C and E at 350° C.

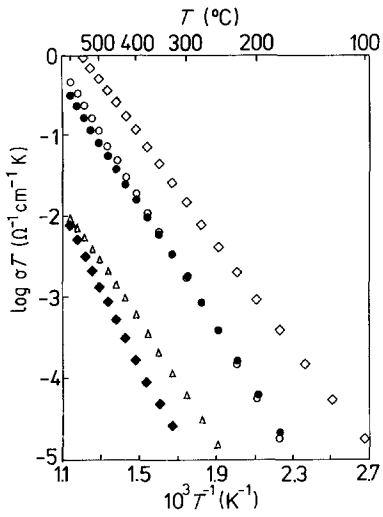

Figure 4 Arrhenius plots for analcime, ○ Li–analcime, △ Rb–analcime, ◇ Na–analcime, ◆ Cs–analcime, ● K–analcime.

employed in determining the bulk resistance. The impedance spectra of all our zeolite specimens showed pronounced minima, hence it was not necessary to employ evaluation techniques.

Experimental data plotted in the complex impedance plane for analcime at different temperatures are shown in Fig. 3. These experimental curves are also typical for all the other investigated zeolites. A characteristic feature is the capacitive contribution of the platinum-blocking electrodes at very low frequencies and the presence of one semi-circle. The separation into two semi-circles as theoretically expected does not appear, for the reason stated above. From the intercept of the spike and the semi-circle, respectively, on the z' axis the overall resistance can be determined. Taking into consideration the geometrical parameters of the pellet the conductivity value may be obtained.

3.2. The activation energies

The activation energy for conductivity can be obtained with the application of Arrhenius plots according to Equation 1 [23]

$$\sigma = (1/T) \times A \times \exp(-\Delta H/RT) \quad (1)$$

In general, ΔH is composed of the energy necessary to generate defect sites in the crystal and the contribution of energy necessary for the ions to overcome potential barriers during migration.

In the temperature range investigated the number of thermally generated defect sites is small in comparison with the number of structurally existing empty sites. This situation is comparable with the "extrinsic" range [23] of ionic crystals. The experimentally determined activation energy represents, together with the foregoing assumption, the value of the potential energy barriers. In plotting ln σT as a function of the inverse of the absolute temperature the activation energy may be determined from the slope of the resulting straight line. As shown in the Arrhenius plots in Fig. 4, the relationship between ln σT and the reciprocal of the absolute temperature is linear over the temperature range given.

Deviations in the activation energies determined for the same zeolite in several measurements extend to $\pm 3\,\mathrm{kJ\,mol^{-1}}$ at maximum. These deviations are mainly due to the pellet preparation process as could be shown in comparison with a series of single crystal measurements and measurements of test circuits.

Data on the ionic conductivities at different temperatures and the activation energies of one representative series of each zeolite are summarized in Table II.

In Figs 5 and 6 the variation of ΔH with cationic radius is shown. There are similar tendencies in analcime, offretite, sodalite (1 : 1) and Ga–sodalite with respect to the variation of ΔH with cationic radius. These zeolites show a pronounced minimum in ΔH for Na^+ ions.

In general, the coulombic attraction between the exchangeable cations and the negatively charged crystal lattice decreases with increasing cation radii. Hence, a decreasing activation energy with increasing cationic radius could be expected. However, this statement is only true for large channel diameters, for example for zeolites with faujasite structure [1]. For channel systems with smaller diameters a steric constriction must be considered. The increasing activation energy in the case of K^+, Rb^+, and Cs^+ ions is due to the steric contribution. Consequently, there should be a continuous increase in activation energy with increasing cationic radius. However, Rb–analcime does not follow this continuous rise, a fact for which we cannot give any explanation. In the case of Rb–sodalite the smaller ΔH value in comparison with K–sodalite is caused by incomplete ion exchange. Only 56% of Na^+ ions were replaced by Rb^+ ions. It is the contribution of the remaining Na^+ ions that leads to a lower activation energy.

A different dependence of ΔH on the cationic radius is shown in Fig. 6 for the silicon-rich sodalite series. The minimum value of ΔH is for the potassium form. Its value is very small in contrast to that of the potassium form of the other sodalites. ΔH of the lithium form of silicon-rich sodalite is much higher in comparison to the corresponding sodalite with an Si/Al ratio of 1 : 1. The following reasons may be given. The negative charges of the lattice in silicon-rich zeolites are at a greater distance from each other than in zeolites with smaller silicon content. This greater distance creates a longer path for the cations when jumping from one site to

TABLE II Ionic conductivities and activation energies of dehydrated zeolites at different temperatures

Zeolite	σ (Ω^{-1} cm^{-1})				ΔH (kJ mol^{-1})
	300° C	400° C	500° C	600° C	
Li-analcime	3.1×10^{-6}	2.8×10^{-5}	1.5×10^{-4}	5.4×10^{-4}	77
Na-analcime	2.6×10^{-5}	1.8×10^{-4}	6.7×10^{-4}	1.9×10^{-3}	63
K-analcime	3.0×10^{-6}	2.4×10^{-5}	1.0×10^{-4}	3.6×10^{-4}	73
Rb-analcime	1.0×10^{-7}	8.7×10^{-7}	3.7×10^{-6}	1.0×10^{-5}	70
Cs-analcime	–	2.6×10^{-7}	1.7×10^{-6}	8.7×10^{-6}	90
Li-sodalite (1 : 1)	1.6×10^{-6}	1.7×10^{-5}	9.1×10^{-5}	4.0×10^{-4}	80
Na-sodalite (1 : 1)	2.2×10^{-6}	1.8×10^{-5}	8.4×10^{-5}	3.2×10^{-4}	72
K-sodalite (1 : 1)	2.4×10^{-6}	4.1×10^{-5}	3.1×10^{-4}	1.3×10^{-3}	93
Rb-sodalite (1 : 1)	4.5×10^{-7}	6.2×10^{-6}	5.0×10^{-5}	2.0×10^{-4}	91
Li-sodalite (5 : 1)	9.1×10^{-8}	1.4×10^{-6}	1.0×10^{-5}	4.5×10^{-5}	92
Na-sodalite (5 : 1)	2.9×10^{-7}	3.7×10^{-6}	2.2×10^{-5}	8.3×10^{-5}	84
K-sodalite (5 : 1)	1.8×10^{-6}	1.4×10^{-5}	6.3×10^{-5}	1.6×10^{-4}	69
Rb-sodalite (5 : 1)	–	–	1.1×10^{-7}	3.9×10^{-7}	82
Li-Ga-sodalite	6.6×10^{-7}	7.6×10^{-6}	3.9×10^{-5}	–	82
Na-Ga-sodalite	2.4×10^{-6}	2.3×10^{-5}	1.5×10^{-4}	8.7×10^{-4}	81
K-Ga-sodalite	3.7×10^{-7}	5.5×10^{-6}	4.5×10^{-5}	2.6×10^{-4}	93
Rb-Ga-sodalite	1.3×10^{-7}	2.1×10^{-6}	2.1×10^{-5}	1.4×10^{-4}	101
Li-offretite	1.1×10^{-6}	1.2×10^{-5}	7.0×10^{-5}	2.5×10^{-4}	82
Na-offretite	9.9×10^{-6}	7.3×10^{-5}	2.4×10^{-4}	5.8×10^{-4}	61
K-offretite	1.5×10^{-6}	1.2×10^{-5}	6.4×10^{-5}	2.0×10^{-4}	74
Rb-offretite	5.7×10^{-7}	6.3×10^{-6}	4.1×10^{-5}	1.7×10^{-4}	84

another which is accompanied by a rise in ΔH. Besides electrostatic forces between ion and lattice and sterical effects a third contribution must be taken into account in the discussion of the activation energy of ionic conductivity. This is the intercationic repulsion which increases with increasing cationic radius in the case of equal cation concentration. For silicon-rich sodalite the cation density is only 1/3 of that in sodalites with Si/Al and Si/Ga, both of which are 1 : 1. Consequently, there is a smaller contribution of intercationic repulsion in silicon-rich sodalite as is shown in Fig. 6 by a continuous decrease in ΔH up to the potassium form. The rise in ΔH for the larger Rb^+ ion may be attributed to increasing sterical effects.

3.3. Ionic conductivities

Assuming similar grain-boundary effects in all the zeolite samples because of uniform sample preparation and pretreatment ionic conductivity values (Table II) are influenced by the zeolitic structure in the following way.

Analcime with its relatively uniform channel structure without pronounced potential wells, such as the β-cages in sodalite, promotes the ionic migration of the small Li^+ and Na^+ ions. Therefore, ionic conductivity values for Li^+ and Na^+ in analcime are better in comparison with sodalite (1 : 1). Only for the bigger K^+ and Rb^+ ions where sterical effects are of increasing influence, do ionic conductivities in sodalite (1 : 1) approach those in analcime or are they somewhat better.

The more compact structure of analcime promotes somewhat better ionic conductivity values for Li^+,

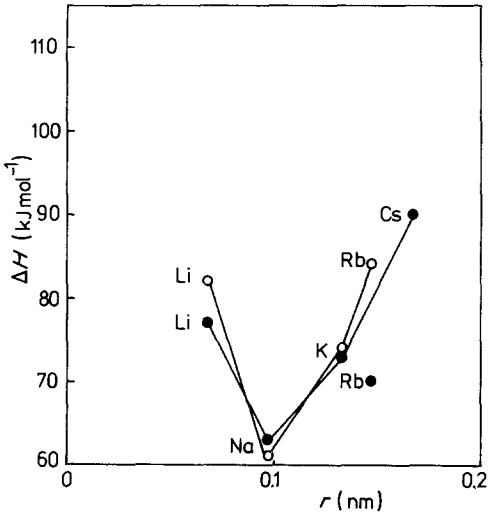

Figure 5 The dependence of ΔH on the radius of the cation for analcime (●) and offretite (○).

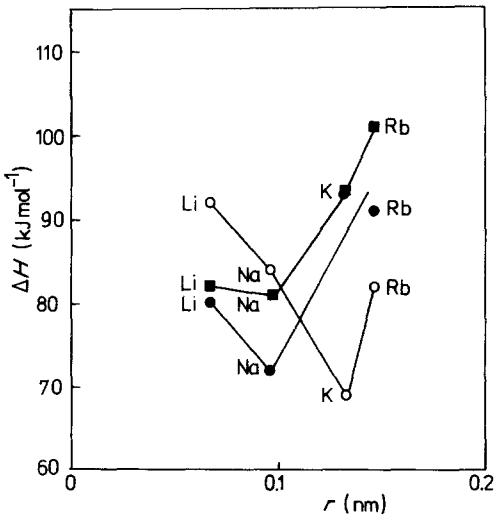

Figure 6 The dependence of ΔH on the radius of the cation for sodalite (1 : 1) (●), silicon-rich sodalite (5 : 1) (○) and Ga-sodalite (■).

Na^+, and K^+ in comparison with offretite. There is a stronger electrostatic interaction between cations and the negatively charged framework in the relatively large channels parallel to the c axis in offretite which counteracts ion migration. Only for the large Rb^+ ion do sterical relations cause somewhat better conductivities in offretite than in analcime. The experimental Na^+ conductivity in zeolite Y, a zeolite with a relatively large channel system, was determined to be in the range between 5×10^{-9} and $7.5 \times 10^{-8}\,\Omega^{-1}\,cm^{-1}$ at 400° C [3]. This conductivity is three orders of magnitude lower in comparison with the values for ionic conductivity in the zeolites used in our investigations. However, in making comparisons one must keep in mind differences in the experimental procedures, including sample preparation and pretreatment, and in the method for determining ionic conductivities from a.c. measurements.

Zeolite A shows a Na^+ conductivity of $4.7 \times 10^{-4}\,\Omega^{-1}\,cm^{-1}$ at 400° C [7] as measured in our laboratories in the frequency range 10 Hz to 10 MHz and determined with the complex plane method. This value of ionic conductivity is somewhat better than that of analcime.

Li-analcime and Li-sodalite show the best Li^+ ion conductivities with $2.8 \times 10^{-5}\,\Omega^{-1}\,cm^{-1}$ and $1.7 \times 10^{-5}\,\Omega^{-1}\,cm^{-1}$ at 400° C. The Li^+ conductivity of analcime and sodalite is comparable to that in lithium germanates (Li_2GeO_3: $1.5 \times 10^{-5}\,\Omega^{-1}\,cm^{-1}$ at 400° C [24]) and is better than that in lithium zincate (Li_6ZnO_4: $5.8 \times 10^{-7}\,\Omega^{-1}\,cm^{-1}$ at 400° C [25]).

The best Na^+ conductivity is shown by Na-analcime with $2.0 \times 10^{-6}\,\Omega^{-1}\,cm^{-1}$ at 200° C which is comparable to the ionic conductivity in $Na_{0.8}In_{0.8}Zr_{0.2}S_2$ with $4 \times 10^{-6}\,\Omega^{-1}\,cm^{-1}$ at 200° C [25].

For K^+ ions the best conductivity value is found in sodalite which is $7.1 \times 10^{-5}\,\Omega^{-1}\,cm^{-1}$ at 425° C. This value is greater in comparison with KF/AlF_3 complexes (K_2AlF_5: $1.5 \times 10^{-5}\,\Omega^{-1}\,cm^{-1}$ and K_3AlF_6: $2 \times 10^{-5}\,\Omega^{-1}\,cm^{-1}$ at 425° C [26]).

However, in comparison with well known alkali-ion conductors such as β-alumina, the ionic conductivity in analcime, sodalite and offretite is several orders of magnitude lower.

At present we are working on a further improvement of the ionic conductivity in dehydrated zeolites. This seems to be possible by carefully directed variation of electrostatical and sterical relations between zeolite framework and migrating ions. Preference will be given to more compact structures as a result of our experiments up to the present.

Acknowledgements

We wish to thank Mrs A. Thöneböhn and Mrs S. Rosenberg for their assistance in synthesizing and analysing zeolites. This work was supported by the Federal Office of Research and Technology of the Federal Republic of Germany under Contract No 03E8565A. The content of this article is the authors own responsibility.

References

1. D. C. FREEMAN JR and D. N. STAMIRES, *J. Chem. Phys.* **35** (1961) 799.
2. D. N. STAMIRES, *ibid.* **36** (1962) 3174.
3. R. A. SCHOONHEYT, in Proceedings of the Fifth International Conference on Zeolites, Naples, Italy, June 1980, edited by L. V. C. Rees (Heyden, London, 1980) p. 242.
4. R. A. SCHOONHEYDT and J. B. UYTTERHOEVEN, in "Molecular Sieve Zeolites I" (American Chemical Society, Washington, D.C., 1971) p. 456.
5. R. A. SCHOONHEYDT and W. DE WILDE, *J. Chem. Soc. Faraday Trans. I* **70** (1974) 2132.
6. R. A. SCHOONHEYDT and F. VELGHE, *ibid.* **72** (1976) 172.
7. W. LORTZ, PhD Thesis, University of Essen (1987).
8. J. H. RAEDER, *Zeolites* **4** (1984) 311.
9. R. AIELLO, R. M. BARRER, J. A. DAVIE and I. S. KERR, *Trans. Faraday Soc.* **66** (1970) 1610.
10. R. SCHMIDT and G. SCHÖN, *Thermochimica Acta* **57** (1982) 125.
11. W. LORTZ, W. OSSWALD, G. KELEMEN and G. SCHÖN, submitted to *J. Phys. E: Sci. Instrum.*
12. J. E. BAUERLE, *J. Phys. Chem. Solids* **30** (1969) 2657.
13. E. WARBURG, *Ann. Phys. Chem.* **67** (1899) 493.
14. *Idem, ibid.* **6** (1901) 125.
15. A. K. JONSCHER, *Phys. Status Solidi* **A32** (1975) 665.
16. R. L. HURT and J. R. MAC DONALD, *Solid State Ionics* **20** (1986) 111.
17. I. M. HODGE, M. D. INGRAM and A. R. WEST, *J. Electroanal. Chem.* **74** (1976) 125.
18. R. D. ARMSTRONG, T. DICKINSON and P. M. WILLIS, *Electroanal. Chem.* **53** (1974) 389.
19. A. K. JONSCHER, *J. Mater. Sci.* **13** (1978) 553.
20. P. H. BOTTELBERGHS, in "Solid Electrolytes" (Academic Press, New York, 1978) p. 145.
21. Y.-T. TSAI, D. H. WHITMORE, *Solid State Ionics* **7** (1982) 129.
22. J. R. MAC DONALD, J. SCHOOMAN and A. P. LEHNEN, *J. Electroanal. Chem.* **131** (1982) 77.
23. R. J. FRIAUF, in "Physics of Electrolytes" Vol. I (Academic Press, London, 1972) p. 153.
24. B. E. LIEBERT and R. A. HUGGINS, *Mater. Res. Bull.* **11** (1976) 533.
25. L. TRICHET and J. ROUXEL, *ibid.* **12** (1977) 345.
26. J. SCHOONMAN, E. E. HELLSTROM and R. A. HUGGINS, *J. Solid State Chem.* **18** (1976) 325.

Received 28 December 1987
and accepted 6 May 1988